

Transport and Burial of Microplastics in Deep-Marine Sediments by Turbidity Currents

Florian Pohl,* Joris T. Eggenhuisen, Ian A. Kane, and Michael A. Clare



Cite This: *Environ. Sci. Technol.* 2020, 54, 4180–4189



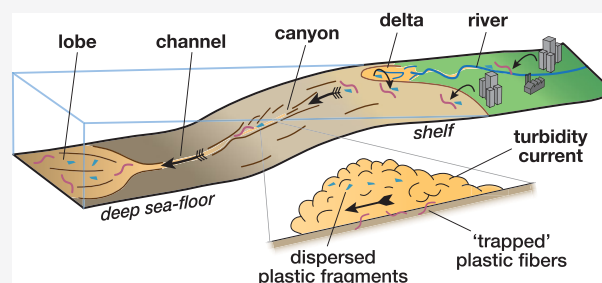
Read Online

ACCESS |

Metrics & More

Article Recommendations

ABSTRACT: The threat posed by plastic pollution to marine ecosystems and human health is under increasing scrutiny. Much of the macro- and microplastic in the ocean ends up on the seafloor, with some of the highest concentrations reported in submarine canyons that intersect the continental shelf and directly connect to terrestrial plastic sources. Gravity-driven avalanches, known as turbidity currents, are the primary process for delivering terrestrial sediment and organic carbon to the deep sea through submarine canyons. However, the ability of turbidity currents to transport and bury plastics is essentially unstudied. Using flume experiments, we investigate how turbidity currents transport microplastics, and their role in differential burial of microplastic fragments and fibers. We show that microplastic fragments become relatively concentrated within the base of turbidity currents, whereas fibers are more homogeneously distributed throughout the flow. Surprisingly, the resultant deposits show an opposing trend, as they are enriched with fibers, rather than fragments. We explain this apparent contradiction by a depositional mechanism whereby fibers are preferentially removed from suspension and buried in the deposits as they are trapped between settling sand-grains. Our results suggest that turbidity currents potentially distribute and bury large quantities of microplastics in seafloor sediments.



INTRODUCTION

The global input of plastic waste into the oceans is estimated to be ~10 million tons per year^{1,2} and is predicted to rise by 1 order of magnitude by 2025.³ Plastics in the marine environment can cause harm to the structure and function of ecosystems.⁴ The component of the ocean plastic budget that comprises microplastics (estimated as 16%,⁵ either manufactured or derived from the breakdown of macroplastics⁶) is of particular growing concern, as microplastics are readily ingested by organisms, can be transferred across the food chain, and may transmit adsorbed or integral toxins such as plasticizers, persistent organic pollutants, and endocrine disruptors on to humans.^{7,8}

To date, most studies have focused on sea surface accumulations of plastics, largely concentrated by currents within the five “great garbage patches” on the sea surface.^{4,9} These sea surface accumulations only account for <1% of the known marine plastics budget,⁵ however, and the remainder is most likely in the deep sea.^{10,11} Recent seafloor sampling has identified plastics, including microplastics, in marine environments ranging from shallow to the deepest locations on the planet.^{10,12,13} The seafloor is therefore an important sink for ocean plastics, including microplastics.^{5,10}

It is important to understand how microplastics are transported to different marine seafloor environments, as many settings where microplastics have been found at seafloor

(e.g., submarine canyons,^{12,14} trenches,^{15,16} seamounts¹⁴) host important but vulnerable deep-sea benthic communities that underpin ocean ecosystems.^{17–23} The exposure level of these ecosystems is determined by the incoming microplastics flux, their residence time, and burial efficiency.²⁴

Seafloor sampling reveals that submarine canyons are sites of preferential plastic accumulation; featuring approximately twice the documented concentrations of open slope, continental shelf, and abyssal plain settings.^{13,25} Submarine canyons are conduits for gravity-driven avalanches of sediment called turbidity currents, which are known to be highly efficient agents for transferring sediment and organic carbon from shallow to deep water.^{26,27} These often-powerful seafloor flows occur when sediment particles are suspended above the seafloor by waves, storms, incoming river plumes, or undersea landslides, and the turbid and relatively dense seawater cascades down the continental slope due to the pull of gravity.^{28–30} Turbidity currents can last for several days, travel

Received: December 11, 2019

Revised: March 4, 2020

Accepted: March 6, 2020

Published: March 6, 2020



over 1000s of km, and transport prodigious volumes of sand as well as cohesive particles of clay and silt with associated compounds (e.g., organic carbon,^{26,29} nutrients and contaminants^{31,32}). Many of these fine-grained particles share hydraulic equivalence with some microplastics.^{13,29,33–36} Deposits resulting from turbidity currents form some of the world's largest sediment accumulations; hence, it has been proposed that turbidity currents may play a role in the dispersal or concentration of microplastics in the deep sea.^{13,24,37}

Using laboratory modeling, we investigate whether turbidity currents act as agents of dispersal or accumulation of microplastics. We pose three specific questions: (1) How are microplastic fragments and fibers transported and distributed within a turbidity current? (2) How effectively do turbidity currents sequester different types of microplastic into seafloor deposits? (3) Where should we expect to find microplastics hotspots within deep-sea submarine depositional-systems and what are the implications for the long-term burial and storage of microplastics?

MATERIALS AND METHODS

Experimental Setup and Procedure. To investigate the transport and burial of microplastics by turbidity currents, microplastic fragments and fibers were added to scaled turbidity currents in flume experiments. The turbidity currents are scaled down from natural to experimental size by applying the theory of hydrodynamic similarity of sediment mobility^{38–40} to turbidity current experiments.^{41,42,89} This scaling approach was termed *Shields scaling* by de Leeuw et al. (2016).⁴¹ For Shields scaling, the sediment transport regime of the experimental currents (characterized by the particle Reynolds number and the Shields parameter) is kept similar to that reported for natural turbidity currents.^{41,42} In the experiments, this can be achieved by adjusting the slope, the sediment concentration, and the flow rate of the experimental turbidity current. To study the behavior of microplastic particles in a turbidity current, the density ratios between the suspended sediment, microplastics, and water, as well as their particle size, should be equal or close to that occurring in nature. The sediment used in the experiments was quartz sand with a density of 2.65 g/cm³. The microplastics added to the turbidity currents have densities of 1.5 g/cm³ for the melamine fragments and 1.38 g/cm³ for the polyester fibers. The quartz sand has a grain-size range similar to that encountered in natural turbidite systems ($d_{10} = 35 \mu\text{m}$, $d_{50} = 133 \mu\text{m}$, $d_{90} = 214 \mu\text{m}$).^{42,89} The melamine fragments have a median size of 200–300 μm , and the polyester fibers have a length of 6 mm and a diameter of 12.5 μm (Figure 1A,B). Our experiments do not include cohesive clay, which would complicate scaling considerably;⁴³ hence, our approach does not take into account cohesive particle interactions,⁴⁴ flocculation processes,^{45,46} or particle support by elasticity.⁴⁷ It is also noted that our experiments do not include interfacial forces that act between the microplastics and the sand grains. However, by using only quartz sand and no cohesive clay, our experiments appropriately represent turbidity currents in sand-dominated canyon systems, such as the well-studied Monterey Canyon offshore California,^{30,48,49} that typify many of the world's continental slopes^{50,51} and have been observed to be active conduits for shallow-deep-sea sediment transport.^{48,49,52,53}

Our aim was to analyze the microplastic content in sediment samples collected from turbidity currents and the resultant

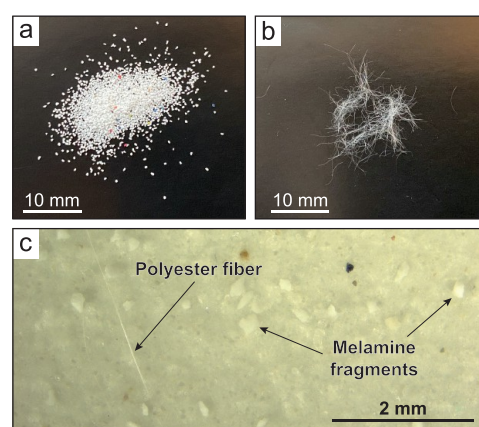


Figure 1. Microplastic melamine-fragments (a) and polyester fibers (b) used in the experiments. Melamine fragments and polyester fibers on a filter paper (c) after the high-density-fluid settling separation.

deposits. To achieve this, two experiments were conducted in a 4 m × 0.5 m × 0.2 m (length × height × width) flume tank filled with fresh water (Figure 2). In the first experiment, sediment samples were collected by siphoning from within the turbidity current. This experiment was conducted with an 8° inclined flume-tank floor, resulting in a completely “bypassing” turbidity current (*sensu* Stevenson et al. (2015)⁵⁴) that left no sediment in the flume tank. Bypassing conditions are necessary to ensure optimal siphon sampling conditions, as a depositional turbidity current would bury the siphon tubes during sampling. Therefore, a second experiment was conducted on a lower angle flume-tank floor of 4°, resulting in a turbidity current that deposited part of its sediment load on the flume-tank floor. It should be noted that while these slope angles are steeper than that encountered in most natural canyon systems, steeper slopes are necessary in Shields scaled experiments to achieve similarity of sediment transport and deposition between the scaled-down flows and nature.^{41,42}

To generate the turbidity currents, a mixture of sediment and fresh water with a volume of 0.45 m³ was prepared in a mixing tank. The sediment concentration in the mixture was set to 15%Vol, or a bulk density of 1.25 g/cm³. To this mixture, 49 g of melamine fragments and 4 g of polyester fibers were added, which resulted in approximately 200 fragments and 100 fibers in 10 g of sediment (Table 1). The mixture was vigorously mixed for 2 min to ensure a homogeneous distribution of microplastics. The short exposure of the microplastics with the sand/water mixture of about 2 min before the start of the experiment, reduces the effect of possible chemical or biological reactions (e.g., degradation or biofouling). To account for any potential background environmental plastic contamination and to measure the exact microplastics concentrations of the mixture, the mixture was siphon-sampled before and after the microplastics were added. After its preparation, the mixture was pumped at a controlled discharge of 12.5 m³/h into the flume tank through an inlet box (Figure 2). The turbidity current flowed through the flume tank driven by gravity acting on its excess density and left the flume through a free overfall into an expansion tank (Figure 2), where it expanded freely and diminished. The duration of an experiment was ca. 100 s until the mixing tank was drained.

During the experiment on the 8° slope, sediment samples of the turbidity current were collected by siphoning, and the flow velocity was monitored with an Ultrasonic Velocity Probe

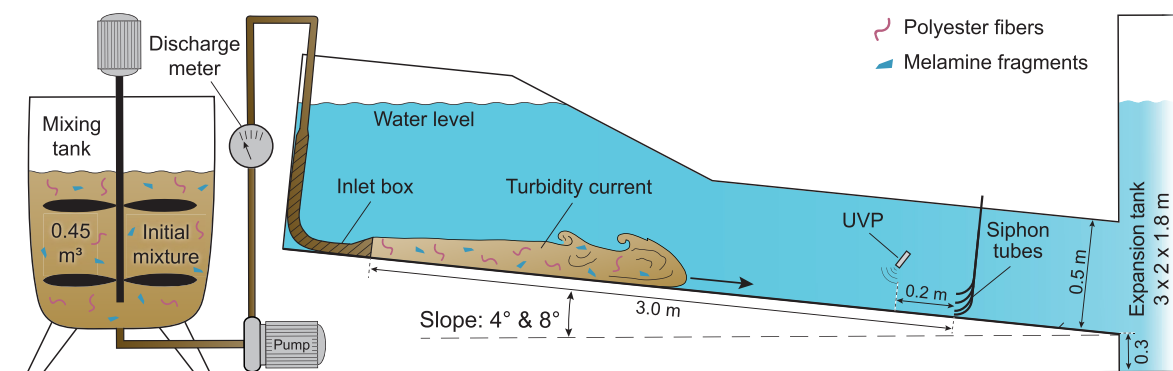


Figure 2. Sketch of the experiment setup. The slope of the flume-tank floor can be adjusted to 4° and 8°. The turbidity current was monitored by an Ultrasonic Velocity Probe (UVP) and sampled with siphon tubes.

Table 1. Results of the Siphon Sampling and the Microplastics Quantification

Sample	Flume-tank floor [deg]	Sampling location	Height above the bed [cm]	Sample vol [ml]	Sediment conc (C) [%Vol]	Sediment wt (w) [g]	Counted microplastics (n_p)		No. of plastics per standard sample volume (C_p)	
							Melamine fragments	Polyester fibers	Melamine fragments	Polyester fibers
1	8	Mixture		27.9	15.0	11.1	194	97	6.95	3.40
2	8	Mixture		26.9	15.0	10.7	178	95	6.61	3.83
3	8	Siphon	8	555.7	0.7	10.5	48	94	0.09	0.17
4	8	Siphon	4	91.5	4.2	10.3	119	58	1.30	0.63
5	8	Siphon	2	36.4	11.8	11.4	119	35	3.26	0.96
6	8	Siphon	1	19.3	20.3	10.4	130	29	6.73	1.50
7	4	Mixture		28.2	15.0	11.2	204	103	7.24	3.44
8	4	Deposits	-1	6.5	60.0	10.4	28	43	4.28	6.57
9	4	Deposits	-2	6.5	60.0	10.4	19	29	2.90	4.43
10	4	Deposits	-3	6.5	60.0	10.3	17	35	2.62	5.40

(UVP; Figure 2). The UVP was positioned 2.8 m downstream of the inlet box and 0.11 m above the flume-tank floor, angled 60° relative to the local bed slope. Siphoning was conducted 3 m downstream of the inlet (i.e., 0.2 m downstream of the UVP) at four different elevations above the flume-tank floor (1, 2, 4, and 8 cm). The inner diameter of the siphon tubes was 7 mm. Siphoning commenced 10 s after the turbidity current entered the flume tank to sample the body of the flow. Siphoning was continued for ~50 s until 2 L was collected from each siphon. The volume and weight of each siphon-tube sample was measured, and sediment concentration was calculated from the bulk density of the sample and the specific densities of the water and sediment. The siphon-tube sample containers were immediately covered and stored for >4 h until all sediments and microplastics had settled. After settling, the melamine fragments and polyester fibers, lying on the top of the sediment, were clearly visible. Clear water was slowly removed with a small hose connected to a slow-moving rotary-pump. This was done with extra caution to ensure that no melamine fragments and polyester fibers were accidentally removed with the water. The concentration of melamine fragments and polyester fibers in the siphon-tube samples was measured by optical microscopy (see section [Microplastic extraction](#)).

After the experiment was run on the 4° slope, deposit thickness was measured through the glass side wall and the flume tank was slowly drained to expose the deposits. Visual inspection through the side glass wall revealed that the thickness of the deposits was constant over the width of the 10

cm wide channel. A vertical section of the deposits was sampled 1.8 m downstream of the inlet box. Samples were collected with a metal spoon. The vertical sampling interval was 1 cm. Approximately 100 g of sediment was collected for each sample. The samples collected from the deposit were also analyzed for their microplastic concentrations.

Microplastic Extraction. Sediment samples were handled in a clean lab by individuals wearing only natural fiber clothing (cotton laboratory coats and headwear) and latex gloves following Woodall et al. (2014).¹⁴ A subsample with a wet-weight of 10.3–11.2 g was extracted from each of the sediment samples with a small metal spoon (Table 1). Prior to subsampling, the sediment samples were vigorously mixed to ensure homogenization of the sample. Microplastics were separated from the quartz sediment using a high-density-fluid settling approach. ZnCl₂ solution with a density of 1.7 g/cm³ was used to ensure sufficient separation of the quartz grains (2.65 g/cm³) from the microplastics (1.35 and 1.5 g/cm³). Settling was conducted in a Sediment-Microplastic-Isolation unit (settling tube with ball valve to isolate the floating microplastics) following the protocol of Coppock et al. (2017),⁵⁵ which was specifically developed for microplastic extraction. Prior to use, the Sediment-Microplastic-Isolation unit was thoroughly rinsed with deionized water. After the settling of the quartz grains to the bottom of the unit, the ball valve was closed and the fluid containing the microplastics was poured and vacuum filtered over a 20 μm filter. In addition, the Sediment-Microplastic-Isolation unit was rinsed with deionized water to flush any remaining microplastics. The filter papers

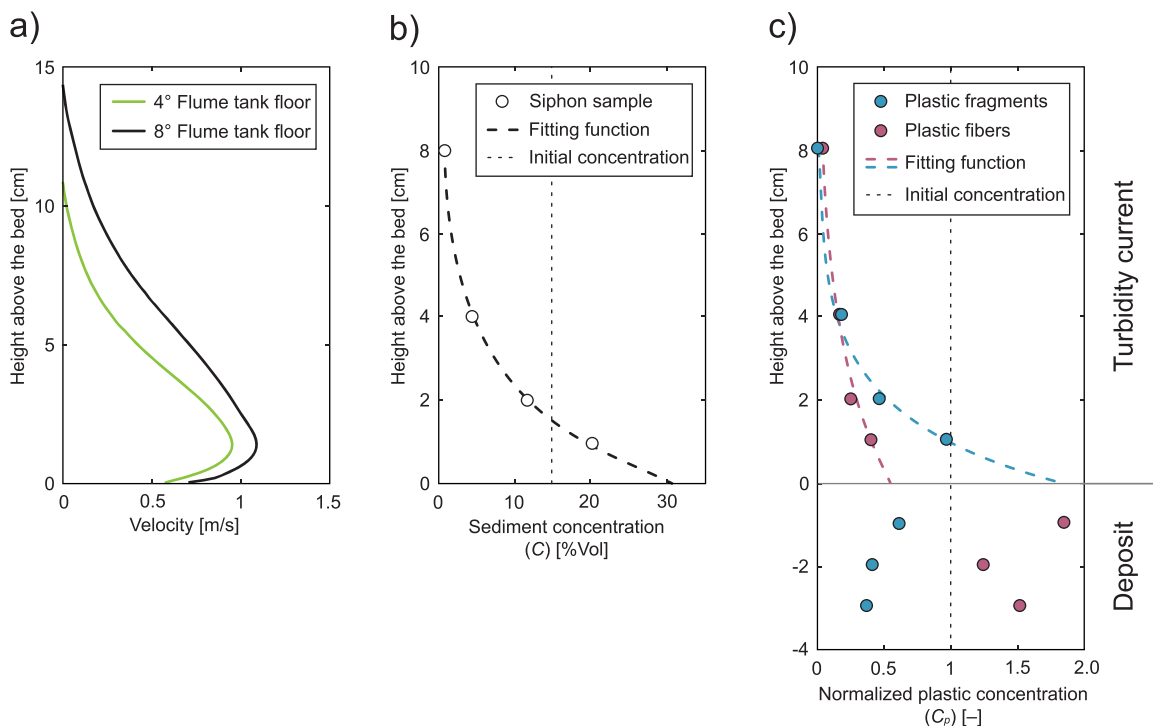


Figure 3. Velocity profiles of the turbidity current (a) measured by the Ultrasonic Velocity Probe located 2.8 m downstream of the inlet box. Vertical sediment concentration per volume of the turbidity current (b). Concentration of melamine fragments and polyester fibers (c) in the turbidity current and in the deposits. Values are normalized with the initial concentrations in the mixing tank.

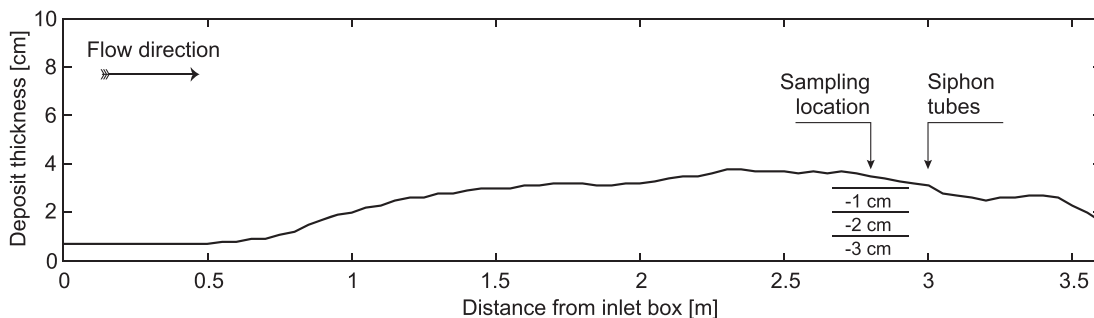


Figure 4. Thickness of the deposits on the flume-tank floor. A vertical section of the deposits was sampled 2.8 m downstream of the inlet box (i.e., 0.2 m in front of the siphon tubes).

were placed on a glass Petri dish, immediately covered, and dried for further analysis by optical microscopy. Optical microscopy was performed using a Zeiss Axio Zoom-V1 stereomicroscope at 20–50× magnification. Melamine fragments and polyester fibers were clearly visible on the filter paper (Figure 1C). The filter papers were traversed with the microscope to systematically count the total number of melamine fragments and polyester fibers. Analysis of the blank samples from the mixing tank revealed no contamination from the melamine fragments or polyester fibers.

Microplastics Quantification. The number of microplastic fragments or fibers (n_p) per mass of sediment (w) was converted into number of plastic particles per standard sample volume (C_p) with equation

$$C_p = C \cdot \rho \cdot \left(\frac{n_p}{w} \right)$$

where C is the sediment concentration per volume, ρ is the density of the suspended sediment (2.65 g/cm³), and w is the

weight of the sediment sample from which the plastics were extracted. For the sediment samples that were siphoned from the turbidity current, C was the volume concentration of sediment in the turbidity current at the height of each siphon tube. For the deposit samples, the concentration was determined in table-top settling experiments as 60%Vol. The microplastics concentration per volume (C_p) was then normalized by dividing through the input C_p obtained from the mixing tank samples.

RESULTS

Description of the Experimental Turbidity Currents.

The maximum velocities of the turbidity currents in the experiments were 0.9 m/s on the 4° slope and 1.1 m/s on the 8° slope (Figure 3A). On the 4° flume-tank floor, the turbidity current deposited part of its sediment load as it was flowing through the flume tank. The thickness of this deposit increased away from the inlet to a maximum thickness of 3.8 cm (Figure 4). The turbidity current on the 8° flume-tank floor bypassed,

leaving no deposit in the flume tank. Siphoning of the turbidity current in the 8° experiment revealed a vertical stratification of the suspended sediment, which is typical for turbidity currents (Figure 3B).^{56,57}

Vertical Distribution of Microplastics within a Turbidity Current. Microplastic concentrations within the turbidity current were generally lower than the concentration of the initial mixture (Table 1 and Figure 3C). The distribution of microplastics in the flow was vertically stratified with increasing concentrations toward the base of the flow. The vertical distribution of the melamine fragments was more stratified than that of the polyester fibers. In the lower half of the flow, at 1 and 2 cm above the bed, the concentration of melamine fragments was higher than the concentration of polyester fibers (Figure 3C). Only the two samples in the upper part of the flow, at 4 and 8 cm above the bed, show a similar concentration of melamine fragments and polyester fibers. An exponential fitting function through the four measurement points suggests that the concentration of melamine fragments at the base of the flow was twice that of the polyester fibers (Figure 3C).

Distribution of Microplastics within the Resultant Deposit. The deposit in the 4° experiment was sampled 2.8 m downstream of the inlet box at three different depths from the bed top. Relative to the initial microplastics concentrations in the mixing tank, the deposits were enriched in polyester fibers but depleted in melamine fragments (Figure 3C). The relative concentrations of polyester fibers in the deposits was almost twice as high as the concentrations of melamine fragments (Table 1).

DISCUSSION

Transport and Burial of Microplastics by Turbidity Currents. The results of the flume experiments allow us to address the questions of how different types of microplastics are transported and deposited by turbidity currents (i.e., research questions 1 and 2 of this paper). Our experiments demonstrate that turbidity currents can transport microplastics. The vertical concentration of melamine fragments in the turbidity current is higher toward the flow base (Figure 3C). This vertical stratification is comparable to that of fine-grained sediment, such as fine-grained quartz sand, silt, or clay as observed in other experimental,^{56,58} or inferred for natural turbidity currents.^{59–62} Polyester fibers are less stratified and appear to be more homogeneously distributed in the turbidity current (Figure 3C). The difference in the vertical distribution between the microplastic fragments and fibers observed in our experiment thus confirms the vertical distribution of microplastic fragments and fibers as conceptualized by Kane and Clare (2019).¹³

The vertical distribution of sediment within a turbidity current is controlled by turbulence and mixing with the ambient fluid, and by settling of the suspended sediment.^{58,63} The efficiency of these two processes strongly depends on the density and shape of the suspended sediment and thus, of the suspended microplastics. Elongated fibers will settle more slowly than fragments due to their larger surface to volume ratio.^{36,64} In addition, the larger surface to volume ratio of fibers makes it easier for them to be mixed upward by turbulent eddies.⁶⁴ Thus, the vertical concentration of microplastic fragments in a turbidity current is expected to be more stratified than that of microplastic fibers, which is confirmed by our experiments (Figure 3C).

Other factors which can determine the vertical sediment distribution within a turbidity current are grain-to-grain interactions and cohesive forces between suspended particles. Grain-to-grain interactions and mechanical sorting can result in an upward migration of larger grains within the flows.⁶⁵ These mechanical sorting mechanisms may represent an additional factor leading to the more homogeneous distribution of the microplastic fibers in our experiments. However, whether these effects translate though to turbidity current dynamics, remains unknown. The experiments presented in this paper are not designed to quantify the effect of mechanical sorting. The second factor that may influence the vertical sediment distribution is the effect of cohesive forces between suspended particles. In our experiments, noncohesive sand was the dominant mass in suspension, and flows were dominated by noncohesive forces. It should be noted, however, that turbidity currents in natural settings often also contain cohesive materials such as clay, which are likely to affect the suspension and deposition behavior of microplastics.

The resultant deposits of microplastic-laden turbidity currents are enriched in polyester fibers. This is a surprising result, because the slow settling of fibers and the relatively low concentration at the base of the turbidity current would suggest a relatively lower abundance in the deposits. The observed concentration of the polyester fibers in the deposits, however, is twice as high as the concentration of the melamine fragments (Table 1 and Figure 3C). The high abundance of fibers in the deposits cannot be explained with settling as the predominant deposition mechanism alone (i.e., competence-driven deposition), as the slow settling of fibers would result in a lower concentration than that of the faster settling melamine fragments. An alternative depositional mechanism to competence-driven deposition is capacity-driven deposition, where sediment gets deposited because the total sediment concentration at the base of the turbidity current reaches the capacity limit.^{66,67} According to this mechanism, sediment is deposited from suspension regardless of its size and density, and thus, the sediment composition of the deposit would reassemble the composition at the base of the flow. However, this appears not to be the case in our experiments as the concentration of polyester fibers and melamine fragments at the base of the flow in the experiment on the 8° slope is different compared to the concentrations in the deposits beneath the experiment on the 4° slope (Figure 3C). Thus, the depositional mechanism for microplastic fibers in a turbidity current seems to work differently and is not captured sufficiently by either conventional depositional mechanism.

Here, we explain the enrichment of fibers in the deposits with a depositional mechanism whereby fibers are removed from suspension as they are trapped between settling sand grains. Due to the elongated size of the fibers and the very large ratio of surface area to volume, it is more likely that they are impacted and dragged downward by settling sand grains (Figure 5). Thus, fibers that are located close to the base of the flow are more likely to get trapped and buried by depositing sand. Fibers may also only be buried partly, and held captive, before they become completely buried at a later stage (Figure 5). This mechanism results in an enrichment of microplastic fibers in the deposits and eventually in a depletion of fibers in the turbidity current. Thus, turbidity currents and other sediment-laden flows (e.g., in flashy bedload-dominated rivers) that feature rapid deposition of coarse grains may represent an efficient segregation and burying mechanism for microplastic

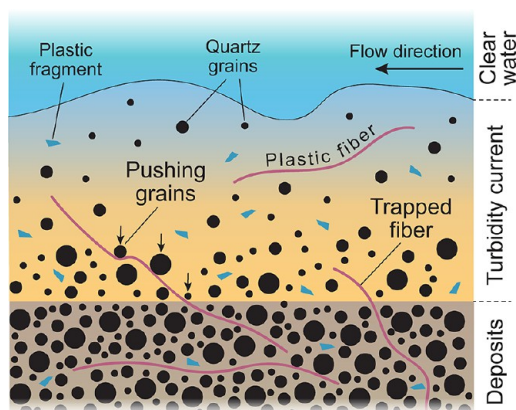


Figure 5. Deposition mechanism of microplastic fragments and fibers in a turbidity current. Fibers are removed from suspension by settling sand grains and become enriched in the deposits. The deposition of the microplastic fragments is more controlled by their low density and high buoyancy resulting in a lower abundance in the deposits. Not to scale.

fibers. However, the depositional mechanism for microplastic fragments is less influenced by the particle shape. Instead, the deposition of fragments is more strongly controlled by their low density, making fragments more likely to stay in suspension and therefore less prone to deposition. This may also explain why we observe lower concentrations of melamine fragments in the deposits than at the base of the turbidity current (Figures 3C and 5).

Implications and Hypotheses for Distribution of Microplastics in Deep-Sea Environments. These specific results of our experiments give rise to a range of predictions

and hypotheses about the distribution and fate of microplastics in deep-sea systems (i.e., research question 3 of this paper). These ideas are discussed here with the aim of identifying possible focus areas for further work in deep-sea microplastics research. The role of the experimental results is thus to direct our thinking about the transport of microplastic in real-world submarine channels (Figure 6).

Terrestrially-sourced plastic litter is transported onto the continental shelf via rivers, deltas, and beaches together with natural sediment (Figure 6).^{68–70} Shelf currents and storm events move plastic litter along the shelf and flush them into the upper part of submarine canyons if present, where plastic accumulates, before being transported further (Figure 6).^{24,69,71,72} Occasionally, sediment stored in the canyon head is remobilized, resulting in the formation of sediment gravity flows, such as debris flows or turbidity currents (Figure 6).⁷³ These flows can flush huge volumes of sediment down the canyon into deeper waters,^{29,74,75} including high concentrations of plastic litter as discovered in canyons in the Messina Strait, South Italy.⁶⁹ Turbidity currents flow down the canyon driven by their excess density, transport their entire sediment load, and can erode into the underlying substrate.^{54,76,77} Thus, turbidity currents will likely entrain and remobilize sediments from the canyon floor including plastic litter. This implies that larger flows are anticipated to re-exhume previously deposited/buried plastic and transport it farther down the system. Due to changes in the local canyon bathymetry, turbidity currents may also deposit part of their sediment load in so-called lag deposits.⁷⁸ Our experiments would suggest that these lag deposits may become enriched in microplastic fibers (Figures 5 and 6).

On the flat abyssal plain at the bottom of the continental slope, turbidity currents build up leveed-channels,⁶⁰ which can

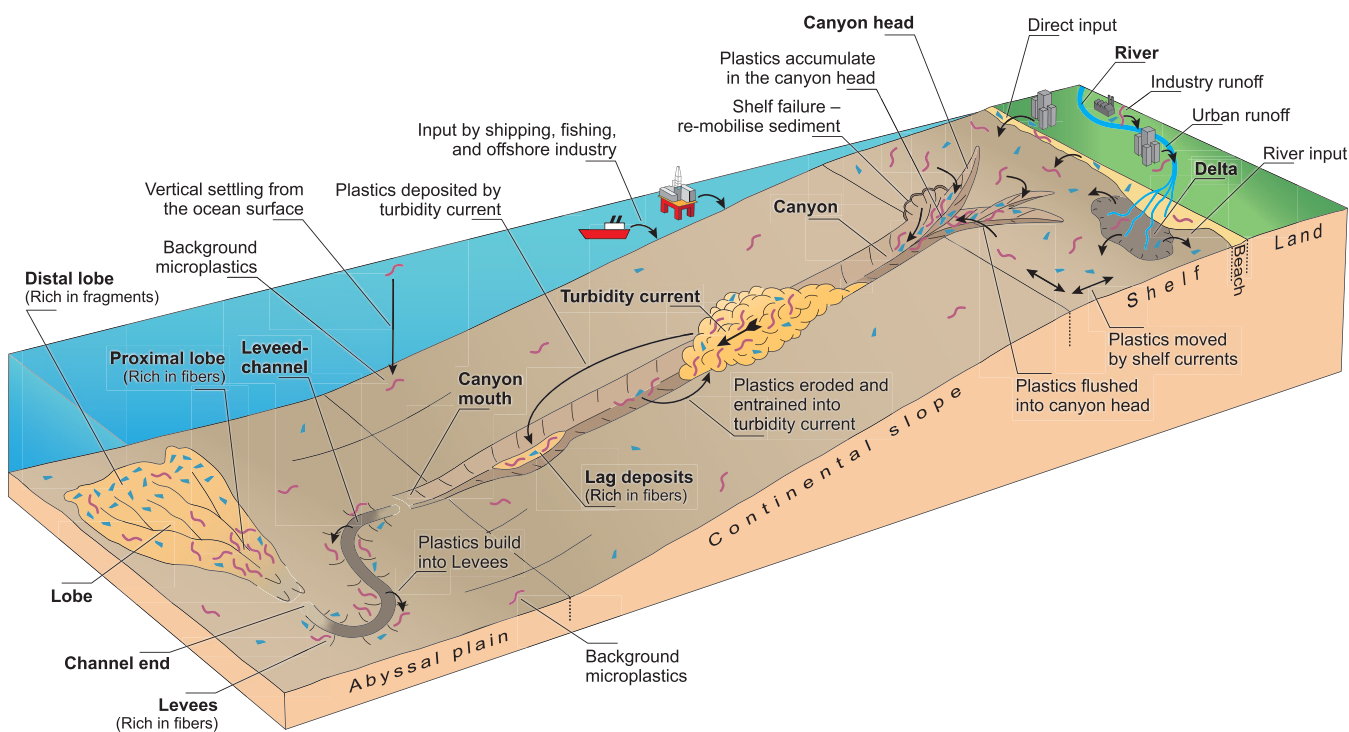


Figure 6. Input pathways of microplastics into the ocean and further transport from the shelf into the deep-marine realm by turbidity currents. Turbidity currents may serve as an efficient segregation and burial mechanism for microplastics resulting in sediments with high microplastic concentrations. Not to scale.

extend over 1000s of kilometers across the ocean floor.⁷⁹ These levees are usually built from sediment that was suspended at the top of the flow.^{59,60,80} On the basis of our experiments, we hypothesize that levee sediments are likely to be rich in microplastic fibers, as the sediment mass suspended at the top of the experimental turbidity currents was rich in microplastic fibers (Table 1). Further down the channel, turbidity currents exit the channel end and deposit lobe-shaped sediment bodies.^{81,82} We hypothesize that the proximal lobe sediments are enriched in microplastic fibers due to their exceptional sedimentation process as discussed above (Figure 5). Due to deposition of fibers in proximal lobe settings, turbidity currents may be depleted in fibers as they flow farther. Thus, the microplastic fragments may become relatively more important in distal lobe deposits (Figure 6).

Our results indicate that turbidity currents will bury a high proportion of the microplastics they carry. Thus, channel, levee, and lobe deposits and hadal trenches that occur at the termination of some deep-sea submarine channels may act as a sink that is highly concentrated in microplastics. The time scales over which this transport arises will depend upon the frequency of the turbidity currents that transit these systems. Some submarine canyon systems, in particular, those that are highly disconnected from sediment inputs in the present-day sea level highstand, feature none or very rare (one per 100 years or more) turbidity currents.¹³ Microplastic transport in such systems is therefore likely to be more strongly controlled by other transport processes, such as internal tides (which can even have a net up-slope advective effect), lateral advection controlled by weak ocean circulation, or vertical settling.^{83,84} We consider systems that are connected directly to sediment input sources, particularly those linked to rivers or that intersect littoral cells on the shelf, to be most likely to transfer microplastics to submarine channels and hence will be most effective for their deep-sea transfer.^{29,30,85} Many such systems have been shown to be very active, with multiple long run-out (>10s of km) turbidity currents occurring within an individual year; hence, these effects are likely to overprint any influence of slow vertical settling on the distribution of microplastic.^{29,30} In particular, sediments on the levees are likely to have much higher microplastic concentrations than pelagic seafloor sediments adjacent to the levee-channel. Benthic organisms, in particular sediment-feeders, living in these microplastic hotspots will be most likely to encounter high microplastic concentrations. The consequences for these organisms are still unknown, but studies have shown that benthic organisms ingest microplastics.^{7,86–88} Furthermore, turbidity currents can segregate microplastic fibers from fragments and generate fiber hotspots (i.e., lag deposits in the canyon or channel thalweg and deposits in the proximal lobe). Benthic organisms in these areas will encounter particularly high concentrations of microplastic fibers. It is noted that microplastic lying on the top of the turbiditic deposits may also be transported further by other processes, such as bottom currents, resulting in further redistribution of microplastics across the seafloor.¹³

Our study underlines the importance of modeling sediment and microplastic-laden flows to understand how turbidity currents may enhance incorporation of microplastics into sediments. Sediment samples from natural turbidity systems are required to test the hypotheses raised in this paper. Sediment traps within canyons, for example, could provide insights into the microplastic distribution within natural turbidity currents. These measurements could also allow us

to quantify the microplastics funneled into deeper water by turbidity currents. Microplastic concentration within the flow should be linked to concentrations in the resultant deposits on the seafloor. Deposit samples should be taken from lag deposits in the canyon or channel thalweg, as well as from the levees and the associated lobe. Many previous studies report microplastic concentrations in seafloor sediments without providing information on the sedimentary subenvironment or the grain size of the host sediment. Such information is essential to understand the nature of past transport processes and hence explain the variations in seafloor microplastic concentrations. Our research provides the first experimental modeling results on the transportation, redistribution, and burial of microplastic by turbidity currents. These results are highly relevant for the planning of sampling and monitoring campaigns in submarine canyon systems in order to understand the dispersal and ultimate fate of microplastics in seafloor sediments.

■ AUTHOR INFORMATION

Corresponding Author

Florian Pohl – Faculty of Geosciences, Utrecht University, 3508TA Utrecht, The Netherlands; Department of Earth Sciences, Durham University, Durham 1DH 3LE, United Kingdom; orcid.org/0000-0003-1008-8467; Email: florian.pohl@durham.ac.uk

Authors

Joris T. Eggenhuisen – Faculty of Geosciences, Utrecht University, 3508TA Utrecht, The Netherlands

Ian A. Kane – School of Earth and Environmental Sciences, University of Manchester, Manchester M13 9PL, United Kingdom

Michael A. Clare – National Oceanography Centre, Southampton SO14 3ZH, United Kingdom

Complete contact information is available at:
<https://pubs.acs.org/10.1021/acs.est.9b07527>

Author Contributions

Experiments were conducted by F. Pohl. Microplastics were separated by F. Pohl and I. Kane. The manuscript was written through contributions of all authors. All authors have given approval to the final version of the manuscript.

Notes

The authors declare no competing financial interest.

■ ACKNOWLEDGMENTS

We thank Thomas Bishop and John Moore in the Department of Geography at The University of Manchester for their help with the microplastics separation. M.C. was supported by the CLASS programme (NERC Grant No. NE/R015953/1). The comments of three anonymous reviewers helped to improve the scope and clarity of the paper.

■ ABBREVIATIONS

UVP, Ultrasonic Velocity Probe

■ REFERENCES

(1) Jambeck, J. R.; Geyer, R.; Wilcox, C.; Siegler, T. R.; Perryman, M.; Andrady, A.; Narayan, R.; Law, K. L. Plastic Waste Inputs from Land into the Ocean. *Science (Washington, DC, U. S.)* **2015**, *347* (6223), 768–771.

- (2) Boucher, J.; Friot, D. *Primary Microplastics in the Oceans: A Global Evaluation of Sources*; IUCN: Gland, Switzerland, 43 pp., 2017. DOI: 10.2305/IUCN.CH.2017.01.en.
- (3) Geyer, R.; Jambeck, J. R.; Law, K. L. Production, Use, and Fate of All Plastics Ever Made. *Sci. Adv.* **2017**, *3* (7), No. e1700782.
- (4) Eriksen, M.; Lebreton, L. C. M.; Carson, H. S.; Thiel, M.; Moore, C. J.; Borerro, J. C.; Galgani, F.; Ryan, P. G.; Reisser, J. Plastic Pollution in the World's Oceans: More than 5 Trillion Plastic Pieces Weighing over 250,000 Tons Afloat at Sea. *PLoS One* **2014**, *9* (12), 1–15.
- (5) Koelmans, A. A.; Kooi, M.; Law, K. L.; van Sebille, E. All Is Not Lost: Deriving a Top-down Mass Budget of Plastic at Sea. *Environ. Res. Lett.* **2017**, *12* (11), 1–9.
- (6) Hartmann, N. B.; Hüffer, T.; Thompson, R. C.; Hassellöv, M.; Verschoor, A.; Daugaard, A. E.; Rist, S.; Karlsson, T.; Brennholt, N.; Cole, M.; Herrling, M. P.; Hess, M. C.; Ivleva, N. P.; Lusher, A. L.; Wagner, M. Are We Speaking the Same Language? Recommendations for a Definition and Categorization Framework for Plastic Debris. *Environ. Sci. Technol.* **2019**, *53* (3), 1039–1047.
- (7) Courtene-Jones, W.; Quinn, B.; Gary, S. F.; Mogg, A. O. M.; Narayanaswamy, B. E. Microplastic Pollution Identified in Deep-Sea Water and Ingested by Benthic Invertebrates in the Rockall Trough, North Atlantic Ocean. *Environ. Pollut.* **2017**, *231*, 271–280.
- (8) Cox, K. D.; Covernton, G. A.; Davies, H. L.; Dower, J. F.; Juanes, F.; Dudas, S. E. Human Consumption of Microplastics. *Environ. Sci. Technol.* **2019**, *53* (12), 7068–7074.
- (9) van Sebille, E.; Wilcox, C.; Lebreton, L.; Maximenko, N.; Hardesty, B. D.; van Franeker, J. A.; Eriksen, M.; Siegel, D.; Galgani, F.; Law, K. L. A Global Inventory of Small Floating Plastic Debris. *Environ. Res. Lett.* **2015**, *10* (12), 124006.
- (10) Thompson, R. C.; Olsen, Y.; Mitchell, R. P.; Davis, A.; Rowland, S. J.; John, A. W. G.; McGonigle, D.; Russell, A. E. Lost at Sea: Where Is All the Plastic? *Science (Washington, DC, U. S.)* **2004**, *304* (5672), 838–838.
- (11) Choy, C. A.; Robison, B. H.; Gagne, T. O.; Erwin, B.; Firl, E.; Halden, R. U.; Hamilton, J. A.; Katija, K.; Lisin, S. E.; Rolsky, C.; Van Houtan, K. S. The Vertical Distribution and Biological Transport of Marine Microplastics across the Epipelagic and Mesopelagic Water Column. *Sci. Rep.* **2019**, *9* (1), 1–9.
- (12) Sanchez-Vidal, A.; Thompson, R. C.; Canals, M.; De Haan, W. P. The Imprint of Microfibres in Southern European Deep Seas. *PLoS One* **2018**, *13* (11), 1–12.
- (13) Kane, I. A.; Clare, M. A. Dispersion, Accumulation and the Ultimate Fate of Microplastics in Deep-Marine Environments: A Review and Future Directions. *Front. Earth Sci.* **2019**, *7* (April), 1–27.
- (14) Woodall, L. C.; Sanchez-Vidal, A.; Canals, M.; Paterson, G. L. J.; Coppock, R.; Sleight, V.; Calafat, A.; Rogers, A. D.; Narayanaswamy, B. E.; Thompson, R. C. The Deep Sea Is a Major Sink for Microplastic Debris. *R. Soc. Open Sci.* **2014**, *1* (4), 140317.
- (15) Bergmann, M.; Wirzberger, V.; Krumpfen, T.; Lorenz, C.; Primpke, S.; Tekman, M. B.; Gerdts, G. High Quantities of Microplastic in Arctic Deep-Sea Sediments from the HAUSGARTEN Observatory. *Environ. Sci. Technol.* **2017**, *51* (19), 11000–11010.
- (16) Fischer, V.; Elsner, N. O.; Brenke, N.; Schwabe, E.; Brandt, A. Plastic Pollution of the Kuril-Kamchatka Trench Area (NW Pacific). *Deep Sea Res., Part II* **2015**, *111*, 399–405.
- (17) Rowe, G. T. The Exploration of Submarine Canyons and Their Benthic Faunal Assemblages. *Proc. - R. Soc. Edinburgh, Sect. B: Biol.* **1972**, *73* (2864), 159–169.
- (18) Hess, S.; Jorissen, F. J. Distribution Patterns of Living Benthic Foraminifera from Cap Breton Canyon, Bay of Biscay: Faunal Response to Sediment Instability. *Deep Sea Res., Part I* **2009**, *56* (9), 1555–1578.
- (19) Vetter, E. W.; Dayton, P. K. Macrofaunal Communities within and Adjacent to a Detritus-Rich Submarine Canyon System. *Deep Sea Res., Part II* **1998**, *45* (1–3), 25–54.
- (20) Boetius, A.; Scheibe, S.; Tselepidis, A.; Thiel, H. Microbial Biomass and Activities in Deep-Sea Sediments of the Eastern Mediterranean: Trenches Are Benthic Hotspots. *Deep Sea Res., Part I* **1996**, *43* (9), 1439–1460.
- (21) Jamieson, A. J.; Fujii, T.; Mayor, D. J.; Solan, M.; Priede, I. G. Hadal Trenches: The Ecology of the Deepest Places on Earth. *Trends Ecol. Evol.* **2010**, *25* (3), 190–197.
- (22) Samadi, S.; Schlacher, T.; de Forges, B. R. Seamount Benthos. In *Seamounts: Ecology, Fisheries & Conservation*; Pitcher, T. J., Morato, T., Hart, P. J. B., Clark, M. R., Haggan, N., Santos, R., Eds.; Blackwell Publishing Ltd: Oxford, UK, 2007; pp 117–140. DOI: 10.1002/9780470691953.ch7.
- (23) Lundsten, L.; Barry, J. P.; Cailliet, G. M.; Clague, D. A.; Devogelaere, A. P.; Geller, J. B. Benthic Invertebrate Communities on Three Seamounts off Southern and Central California, USA. *Mar. Ecol.: Prog. Ser.* **2009**, *374* (1989), 23–32.
- (24) Ballent, A.; Pando, S.; Purser, A.; Juliano, M. F.; Thomsen, L. Modelled Transport of Benthic Marine Microplastic Pollution in the Nazaré Canyon. *Biogeosciences* **2013**, *10* (12), 7957–7970.
- (25) Pham, C. K.; Ramirez-Llodra, E.; Alt, C. H. S.; Amaro, T.; Bergmann, M.; Canals, M.; Company, J. B.; Davies, J.; Duineveld, G.; Galgani, F.; Howell, K. L.; Huvenne, V. A. I.; Isidro, E.; Jones, D. O. B.; Lastras, G.; Morato, T.; Gomes-Pereira, J. N.; Purser, A.; Stewart, H.; Tojeira, I.; Tubau, X.; Van Rooij, D.; Tyler, P. A. Marine Litter Distribution and Density in European Seas, from the Shelves to Deep Basins. *PLoS One* **2014**, *9* (4), 1–13.
- (26) Galy, V.; France-Lanord, C.; Beyssac, O.; Faure, P.; Kudrass, H.; Palhol, F. Efficient Organic Carbon Burial in the Bengal Fan Sustained by the Himalayan Erosional System. *Nature* **2007**, *450* (7168), 407–410.
- (27) Liu, J. T.; Hsu, R. T.; Hung, J. J.; Chang, Y. P.; Wang, Y. H.; Rendle-Bühning, R. H.; Lee, C. L.; Huh, C. A.; Yang, R. J. From the Highest to the Deepest: The Gaoping River-Gaoping Submarine Canyon Dispersal System. *Earth-Sci. Rev.* **2016**, *153*, 274–300.
- (28) Daly, R. A. Origin of Submarine “Canyons”. *Am. J. Sci.* **1936**, *31* (186), 401–420.
- (29) Azpiroz-Zabala, M.; Cartigny, M. J. B.; Talling, P. J.; Parsons, D. R.; Sumner, E. J.; Clare, M. A.; Simmons, S. M.; Cooper, C.; Pope, E. L. Newly Recognized Turbidity Current Structure Can Explain Prolonged Flushing of Submarine Canyons. *Sci. Adv.* **2017**, *3* (10), 1–12.
- (30) Paull, C. K.; Talling, P. J.; Maier, K. L.; Parsons, D.; Xu, J.; Caress, D. W.; Gwiazda, R.; Lundsten, E. M.; Anderson, K.; Barry, J. P.; Chaffey, M.; O'Reilly, T.; Rosenberger, K. J.; Gales, J. A.; Kieft, B.; McGann, M.; Simmons, S. M.; McCann, M.; Sumner, E. J.; Clare, M. A.; Cartigny, M. J. Powerful Turbidity Currents Driven by Dense Basal Layers. *Nat. Commun.* **2018**, *9* (1), 4114.
- (31) Gwiazda, R.; Paull, C. K.; Ussler, W.; Alexander, C. R. Evidence of Modern Fine-Grained Sediment Accumulation in the Monterey Fan from Measurements of the Pesticide DDT and Its Metabolites. *Mar. Geol.* **2015**, *363*, 125–133.
- (32) Fernandez-Arcaya, U.; Ramirez-Llodra, E.; Aguzzi, J.; Allcock, A. L.; Davies, J. S.; Dissanayake, A.; Harris, P.; Howell, K.; Huvenne, V. A. I.; Macmillan-Lawler, M.; Martin, J.; Menot, L.; Nizinski, M.; Puig, P.; Rowden, A. A.; Sanchez, F.; Van den Beld, I. M. J. Ecological Role of Submarine Canyons and Need for Canyon Conservation: A Review. *Front. Mar. Sci.* **2017**, *4*, 1–26.
- (33) Heezen, B. C.; Ewing, M.; Menzies, R. J. The Influence of Submarine Turbidity Currents on Abyssal Productivity. *Oikos* **1955**, *6* (2), 170.
- (34) Stanley, D. J. Turbidity Current Transport of Organic-Rich Sediments: Alpine and Mediterranean Examples. *Mar. Geol.* **1986**, *70* (1–2), 85–101.
- (35) Ballent, A.; Purser, A.; de Jesus Mendes, P.; Pando, S.; Thomsen, L. Physical Transport Properties of Marine Microplastic Pollution. *Biogeosciences Discuss.* **2012**, *9* (12), 18755–18798.
- (36) Khatmullina, L.; Isachenko, I. Settling Velocity of Microplastic Particles of Regular Shapes. *Mar. Pollut. Bull.* **2017**, *114* (2), 871–880.
- (37) Zalasiewicz, J.; Waters, C. N.; Ivar do Sul, J. A.; Corcoran, P. L.; Barnosky, A. D.; Cearreta, A.; Edgeworth, M.; Galuszka, A.; Jeandel,

C.; Leinfelder, R.; McNeill, J. R.; Steffen, W.; Summerhayes, C.; Wagerich, M.; Williams, M.; Wolfe, A. P.; Yonan, Y. The Geological Cycle of Plastics and Their Use as a Stratigraphic Indicator of the Anthropocene. *Anthropocene* **2016**, *13*, 4–17.

(38) Yalin, M. S. *Theory of Hydraulic Models*; Macmillan: London, 1971.

(39) Peakall, J.; Ashworth, P.; Best, J. Physical Modelling in Fluvial Geomorphology: Principles, Applications and Unresolved Issue. In *The Scientific Nature of Geomorphology*; Rhoads, B. L., Thorn, C. E., Eds.; John Wiley and Sons: Chichester, 1996; pp 221–253.

(40) Hughes, S. A. *Physical Models and Laboratory Techniques in Coastal Engineering*; World Scientific: 1993.

(41) de Leeuw, J.; Eggenhuisen, J. T.; Cartigny, M. J. B. Morphodynamics of Submarine Channel Inception Revealed by New Experimental Approach. *Nat. Commun.* **2016**, *7*, 1–7.

(42) Pohl, F.; Eggenhuisen, J. T.; Tilston, M.; Cartigny, M. J. B. New Flow Relaxation Mechanism Explains Scour Fields at the End of Submarine Channels. *Nat. Commun.* **2019**, *10* (1), 4425.

(43) Hermidas, N.; Eggenhuisen, J. T. J. T.; Jacinto, R. S. R. S.; Luthi, S. M. S. M.; Toth, F.; Pohl, F. A Classification of Clay-Rich Subaqueous Density Flow Structures. *J. Geophys. Res.: Earth Surf.* **2018**, *123* (5), 945–966.

(44) Lane-Serff, G. F. Deposition of Cohesive Sediment from Turbulent Plumes, Gravity Currents, and Turbidity Currents. *J. Hydraul. Eng.* **2011**, *137* (12), 1615–1623.

(45) Tran, D.; Strom, K. Suspended Clays and Silts: Are They Independent or Dependent Fractions When It Comes to Settling in a Turbulent Suspension*. *Cont. Shelf Res.* **2017**, *138*, 81–94.

(46) Tran, D.; Strom, K. Floc Sizes and Resuspension Rates from Fresh Deposits: Influences of Suspended Sediment Concentration, Turbulence, and Deposition Time. *Estuarine, Coastal Shelf Sci.* **2019**, *229* (June), 106397.

(47) Hermidas, N.; Silva Jacinto, R.; Eggenhuisen, J. T.; Luthi, S. M. A New Rheological Model for Thixoeastic Materials in Subaqueous Gravity Driven Flows. *J. Non-Newtonian Fluid Mech.* **2019**, *266*, 102–117.

(48) Heerema, C. J.; Talling, P. J.; Cartigny, M. J.; Paull, C. K.; Bailey, L.; Simmons, S. M.; Parsons, D. R.; Clare, M. A.; Gwiazda, R.; Lundsten, E.; Anderson, K.; Maier, K. L.; Xu, J. P.; Sumner, E. J.; Rosenberger, K.; Gales, J.; Mcgann, M.; Carter, L.; Pope, E.; Coordinated, M. What Determines the Downstream Evolution of Turbidity Currents? *Earth Planet. Sci. Lett.* **2020**, *532*, 116023.

(49) Xu, J. P. Normalized Velocity Profiles of Field-Measured Turbidity Currents. *Geology* **2010**, *38* (6), 563–566.

(50) Piper, D. J. W.; Normark, W. R. Sandy Fans—from Amazon to Hueneme and Beyond. *AAPG Bull.* **2001**, *85* (8), 1407–1438.

(51) Nelson, C. H.; Maldonado, A.; Barber, J. H.; Alonso, B. *Modern Sand-Rich and Mud-Rich Siliciclastic Aprons: Alternative Base-of-Slope Turbidite Systems to Submarine Fans* **1991**, 171–190.

(52) Gwiazda, R.; Paull, C. K.; Ussler, W.; Alexander, C. R. Evidence of Modern Fine-Grained Sediment Accumulation in the Monterey Fan from Measurements of the Pesticide DDT and Its Metabolites. *Mar. Geol.* **2015**, *363*, 125–133.

(53) Xu, J. P.; Sequeiros, O. E.; Noble, M. A. Sediment Concentrations, Flow Conditions, and Downstream Evolution of Two Turbidity Currents, Monterey Canyon, USA. *Deep Sea Res., Part I* **2014**, *89*, 11–34.

(54) Stevenson, C. J.; Jackson, C. A.-L.; Hodgson, D. M.; Hubbard, S. M.; Eggenhuisen, J. T. Deep-Water Sediment Bypass. *J. Sediment. Res.* **2015**, *85* (9), 1058–1081.

(55) Coppock, R. L.; Cole, M.; Lindeque, P. K.; Queirós, A. M.; Galloway, T. S. A Small-Scale, Portable Method for Extracting Microplastics from Marine Sediments. *Environ. Pollut.* **2017**, *230*, 829–837.

(56) Garcia, M. H. Depositional Turbidity Currents Laden with Poorly Sorted Sediment. *J. Hydraul. Eng.* **1994**, *120* (11), 1240–1263.

(57) Sequeiros, O. E.; Mosquera, R.; Pedocchi, F. Internal Structure of a Self-Accelerating Turbidity Current. *J. Geophys. Res. Ocean.* **2018**, *123* (9), 6260–6276.

(58) Eggenhuisen, J. T.; Tilston, M. C.; de Leeuw, J.; Pohl, F.; Cartigny, M. J. B. Turbulent Diffusion Modelling of Sediment in Turbidity Currents; an Experimental Validation of the Rouse Approach. *Depos. Rec.* **2020**, *6* (1), 1–14.

(59) Hansen, L. A. S.; Callow, R. H. T.; Kane, I. A.; Gamberi, F.; Rovere, M.; Cronin, B. T.; Kneller, B. C. Genesis and Character of Thin-Bedded Turbidites Associated with Submarine Channels. *Mar. Pet. Geol.* **2015**, *67*, 852–879.

(60) Hiscott, R. N.; Hall, F. R.; Pirmez, C. Turbidity-Current Overspill from the Amazon Channel: Texture of the Silt/Sand Load, Paleoflow from Anisotropy of Magnetic Susceptibility, and Implications for Flow Processes. *Proc. Ocean Drill. Program, Sci. Results* **1997**, *155*, 531–538.

(61) Pirmez, C.; Imran, J. Reconstruction of Turbidity Currents in Amazon Channel. *Mar. Pet. Geol.* **2003**, *20* (6–8), 823–849.

(62) Jobe, Z.; Sylvester, Z.; Pittaluga, M. B.; Frascati, A.; Pirmez, C.; Minisini, D.; Howes, N.; Cantelli, A. Facies Architecture of Submarine Channel Deposits on the Western Niger Delta Slope: Implications for Grain-Size and Density Stratification in Turbidity Currents. *J. Geophys. Res. Earth Surf.* **2017**, *122* (2), 473–491.

(63) Rouse, H. Modern Conceptions of the Mechanics of Fluid Turbulence. *Am. Soc. Civ. Eng. Trans.* **1937**, *102*, 463–543.

(64) Shin, M.; Koch, D. L. Rotational and Translational Dispersion of Fibres in Isotropic Turbulent Flows. *J. Fluid Mech.* **2005**, *540*, 143–173.

(65) Möbius, M. E.; Lauderdale, B. E.; Nagel, S. R.; Jaeger, H. M. Size Separation of Granular Particles. *Nature* **2001**, *414* (6861), 270.

(66) Hiscott, R. N. Loss of Capacity, Not Competence, as the Fundamental Process Governing Deposition from Turbidity Currents. *J. Sediment. Res.* **1994**, *A64* (3), 209–214.

(67) Eggenhuisen, J. T.; Cartigny, M. J. B.; de Leeuw, J. Physical Theory for Near-Bed Turbulent Particle Suspension Capacity. *Earth Surf. Dyn.* **2017**, *5* (2), 269–281.

(68) Lebreton, L. C. M.; Van Der Zwet, J.; Damsteeg, J. W.; Slat, B.; Andrady, A.; Reisser, J. River Plastic Emissions to the World's Oceans. *Nat. Commun.* **2017**, *8*, 1–10.

(69) Pierdomenico, M.; Casalbore, D.; Chiocci, F. L. Massive Benthic Litter Funnelled to Deep Sea by Flash-Flood Generated Hyperpycnal Flows. *Sci. Rep.* **2019**, *9* (1), 1–10.

(70) Moore, C. J.; Lattin, G. L.; Zellers, A. F. Quantity and Type of Plastic Debris Flowing from Two Urban Rivers to Coastal Waters and Beaches of Southern California. *J. Integr. Coast. Zo. Manag.* **2011**, *11*, 65–73.

(71) Mordecai, G.; Tyler, P.; Masson, D. G.; Huvenne, V. Litter in Submarine Canyons off the West Coast of Portugal. *Deep Sea Res., Part II* **2011**, *58*, 2489–2496.

(72) Lattin, G. L.; Moore, C. J.; Zellers, A. F.; Moore, S. L.; Weisberg, S. B. A Comparison of Neustonic Plastic and Zooplankton at Different Depths near the Southern California Shore. *Mar. Pollut. Bull.* **2004**, *49*, 1–4.

(73) Talling, P. J.; Paull, C. K.; Piper, D. J. W. How Are Subaqueous Sediment Density Flows Triggered, What Is Their Internal Structure and How Does It Evolve? Direct Observations from Monitoring of Active Flows. *Earth-Sci. Rev.* **2013**, *125*, 244–287.

(74) Canals, M.; Puig, P.; De Madron, X. D.; Heussner, S.; Palanques, A.; Fabres, J. Flushing Submarine Canyons. *Nature* **2006**, *444* (7117), 354–357.

(75) Mountjoy, J. J.; Howarth, J. D.; Orpin, A. R.; Barnes, P. M.; Bowden, D. A.; Rowden, A. A.; Schimel, A. C. G.; Holden, C.; Horgan, H. J.; Nodder, S. D.; Patton, J. R.; Lamarche, G.; Gerstenberger, M.; Micallef, A.; Palletin, A.; Kane, T. Earthquakes Drive Large-Scale Submarine Canyon Development and Sediment Supply to Deep-Ocean Basins. *Sci. Adv.* **2018**, *4* (3), 1–9.

(76) Pantin, H. M.; Franklin, M. C. Predicting Autosuspension in Steady Turbidity Flow: Ignition Points and Their Relation to Richardson Numbers. *J. Sediment. Res.* **2009**, *79* (12), 862–871.

(77) Parker, G.; Garcia, M.; Fukushima, Y.; Yu, W. Experiments on Turbidity Currents over an Erodible Bed. *J. Hydraul. Res.* **1987**, *25* (1), 123–147.

(78) Zelt, F. B.; Rossen, C. Geometry and Continuity of Deep-Water Sandstones and Siltstones, Brushy Canyon Formation (Permian) Delaware Mountains, Texas. In *Atlas of Deep Water Environments*; Pickering, K. T., Hiscott, R. N., Kenyon, N. H., Ricci Lucchi, F., Smith, R. D. A., Eds.; Springer Netherlands: Dordrecht, 1995; pp 167–183. DOI: 10.1007/978-94-011-1234-5_26.

(79) Klaucke, I.; Hesse, R.; Ryan, W. B. F. F. Morphology and Structure of a Distal Submarine Trunk Channel: The Northwest Atlantic Mid-Ocean Channel between Lat 53°N and 44°30'N. *Geol. Soc. Am. Bull.* **1998**, *110* (1), 22–34.

(80) de Leeuw, J.; Eggenhuisen, J. T.; Sychala, Y. T.; Heijnen, M. S.; Pohl, F.; Cartigny, M. J. B. Sediment Volume and Grain-Size Partitioning Between Submarine Channel-Levee Systems and Lobes: An Experimental Study. *J. Sediment. Res.* **2018**, *88* (7), 777–794.

(81) Prélat, A.; Covault, J. A.; Hodgson, D. M.; Fildani, A.; Flint, S. S. Intrinsic Controls on the Range of Volumes, Morphologies, and Dimensions of Submarine Lobes. *Sediment. Geol.* **2010**, *232* (1–2), 66–76.

(82) Mutti, E.; Normark, W. R. An Integrated Approach to the Study of Turbidite Systems. In *Seismic Facies and Sedimentary Processes of Submarine Fans and Turbidite Systems*; Weimer, P., Link, M. H., Eds.; Springer: New York, 1991; Vol. 1, pp 75–106. DOI: 10.1007/978-1-4684-8276-8_4.

(83) Martín, J.; Palanques, A.; Vitorino, J.; Oliveira, A.; de Stigter, H. C. Near-Bottom Particulate Matter Dynamics in the Nazaré Submarine Canyon under Calm and Stormy Conditions. *Deep Sea Res., Part II* **2011**, *58* (23–24), 2388–2400.

(84) Rebesco, M.; Hernández-Molina, F. J.; Van Rooij, D.; Wählin, A. Contourites and Associated Sediments Controlled by Deep-Water Circulation Processes: State-of-the-Art and Future Considerations. *Mar. Geol.* **2014**, *352*, 111–154.

(85) Hage, S.; Cartigny, M. J. B.; Sumner, E. J.; Clare, M. A.; Hughes Clarke, J. E.; Talling, P. J.; Lintern, D. G.; Simmons, S. M.; Silva Jacinto, R.; Vellinga, A. J.; Allin, J. R.; Azpiroz-Zabala, M.; Gales, J. A.; Hizzett, J. L.; Hunt, J. E.; Mozzato, A.; Parsons, D. R.; Pope, E. L.; Stacey, C. D.; Symons, W. O.; Vardy, M. E.; Watts, C. Direct Monitoring Reveals Initiation of Turbidity Currents From Extremely Dilute River Plumes. *Geophys. Res. Lett.* **2019**, *46* (20), 11310–11320.

(86) Graham, E. R.; Thompson, J. T. Deposit- and Suspension-Feeding Sea Cucumbers (Echinodermata) Ingest Plastic Fragments. *J. Exp. Mar. Biol. Ecol.* **2009**, *368* (1), 22–29.

(87) Hall, N. M.; Berry, K. L. E.; Rintoul, L.; Hoogenboom, M. O. Microplastic Ingestion by Scleractinian Corals. *Mar. Biol.* **2015**, *162*, 725–732.

(88) Taylor, M. L.; Gwinnett, C.; Robinson, L. F.; Woodall, L. C. Plastic Microfibre Ingestion by Deep-Sea Organisms. *Sci. Rep.* **2016**, *6* (May), 1–9.

(89) Pohl, F.; Eggenhuisen, J. T.; Cartigny, M. J. B.; Tilston, M. C.; De Leeuw, J.; Hermidas, N. The influence of a slope break on turbidite deposits: An experimental investigation. *J. Margeo* **2020**, DOI: 10.1016/j.margeo.2020.106160, in press.